



Journal of the Mexican Chemical Society

ISSN: 1870-249X

editor.jmcs@gmail.com

Sociedad Química de México

México

Álvarez-Manzo, Rodolfo; Mendoza-Canales, Joel; Castillo-Cervantes, Salvador; Marín-Cruz, Jesús  
Studies on the Development of New Efficient Corrosion Inhibitors for Crude Oil Pipelines:  
Electrochemical Impedance Spectroscopy Results for 1,8-Naphthyridines  
Journal of the Mexican Chemical Society, vol. 57, núm. 1, enero-marzo, 2013, pp. 30-35  
Sociedad Química de México  
Distrito Federal, México

Available in: <http://www.redalyc.org/articulo.oa?id=47527412007>

- How to cite
- Complete issue
- More information about this article
- Journal's homepage in redalyc.org

redalyc.org

Scientific Information System  
Network of Scientific Journals from Latin America, the Caribbean, Spain and Portugal  
Non-profit academic project, developed under the open access initiative

# Studies on the Development of New Efficient Corrosion Inhibitors for Crude Oil Pipelines: Electrochemical Impedance Spectroscopy Results for 1,8-Naphthyridines

Rodolfo Álvarez-Manzo,\* Joel Mendoza-Canales, Salvador Castillo-Cervantes, and Jesús Marín-Cruz

Instituto Mexicano del Petróleo. Eje Central Lázaro Cárdenas Norte No. 152, Col. San Bartolo Atepehuacan, C. P. 07730, México, D. F. Tel.: +52-55-9175-6402. ramanzo@imp.mx

Received September 3, 2012; accepted March 13, 2013

**Abstract.** Five 1,8-naphthyridines were tested as corrosion inhibitors, including three non-previously reported 3-alkyl-1,8-naphthyridines. All were produced via the extended Friedländer synthesis, that for 3-alkyl-1,8-naphthyridines involves the earliest use of aliphatic aldehydes. Fragmentation pattern in MS for 3-alkyl-1,8-naphthyridines shows a remarkable parallel with that exhibited by 3-alkylpyridines. Electrochemical Impedance Spectroscopy (EIS) was used to assess the inhibiting properties of these compounds on samples of API X52 carbon steel pipelines immersed in oilfield-related water. Except for one of the molecules tested, the inhibition efficiency (IE%) values were significantly higher than that calculated for a reference commercial inhibitor.

**Key words:** 1,8-Naphthyridines, corrosion inhibitor, Friedländer synthesis, electrochemical impedance spectroscopy, inhibition efficiency.

**Resumen.** Se estudiaron cinco 1,8-naftiridinas como inhibidores de corrosión, las cuales incluyen 3-alkil-1,8-naftiridinas no descritas previamente. Todas estas sustancias se prepararon por medio de la extensión de la síntesis de Friedländer, que para las 3-alkil-1,8-naftiridinas involucra el uso, por vez primera, de aldehídos alifáticos. El patrón de fragmentación en espectrometría de masas para las 3-alkil-1,8-naftiridinas muestra un notorio paralelismo con el exhibido por las 3-alkilpiridinas. Se utilizó espectroscopia de impedancia electroquímica (EIE) para evaluar las propiedades inhibitorias de estos compuestos en muestras inmersas en agua congénita de acero al carbono de tuberías API X52. Excepto para una de las moléculas estudiadas, los valores de eficiencia de inhibición (EI%) fueron significativamente más altos que los calculados para un inhibidor comercial de referencia.

**Palabras clave:** 1,8-Naftiridinas, inhibidor de corrosión, síntesis de Friedländer, espectroscopia de impedancia electroquímica, eficiencia de inhibición.

## Introduction

An organic corrosion inhibitor is a compound that decreases the corrosion rate of inner surface of steel pipelines, which is a key subject in oil industry. In the structure of an organic molecule designed to inhibit corrosion two distinct moieties can be recognized: one or several long hydrocarbon or polyether chains (up to 18 atoms), and a “nucleus” or “head” that consists of a functional group or a ring system, often containing heteroatoms with electron lone pairs, such as nitrogen, oxygen and sulfur, to which the chains are attached. Many research efforts have been made focusing primarily on the effect of chain length modification; some of them include structures where the electron donor heteroatom is formally absent. However, the “head” moiety also plays a significant role in the inhibitory activity. It has been suggested that the inhibitor binds to the metal surface through the electron pairs of the heteroatom. This phenomenon alters the electron potential on the metallic surface, thus diminishing the kinetics and eventually the oxidation tendency [1-3]. One of the strategies to counteract the detrimental corrosion effects by way of organic inhibitors is to develop new highly efficient products based on a meticulous examination of their structure. An option is to synthesize molecules structurally related to compounds with proved inhibiting properties, but with a greater number of active sites (that is, heteroatoms) in the “head” moiety. From this perspective, quinolines (**1**, Fig. 1), having remarkable corrosion inhibiting properties in spite

of the absence of long alkyl chains in their structure [4-7], are appealing model compounds.

Therefore, the intention in this work was to synthesize and evaluate a quinoline-related heterocyclic family of compounds with a second electron donor nitrogen atom located in the fused-ring system. The primary strategy was to keep donation from the heteroatoms aligned on the metal surface (with negligible conformational changes) in order to promote the inhibitor-metal surface bond. Therefore, a decision was made to analyze the 1,8-naphthyridine ring **2** [8-10] (basic ring  $R = R' = H$ ). In this study two groups of compounds were taken into consideration: Group I or classical 1,8-naphthyridines (**2a** and **2b**, Fig. 1), and Group II or 3-alkyl-1,8-naphthyridines (**2c-e**), without substitution in C-2 to prevent any steric hindrance factor that precludes the expected bonding to the metal surface, and a linear alkyl chain in C-3 as the other key component, the latter based on the typical structure of many organic inhibitors.

There are several synthetic routes for the 1,8-naphthyridine ring; one of the most frequently used is the extension of the Friedländer synthesis [11], that involves the utilization of 2-aminonicotinaldehyde **3** [12] and an active methylene component [13]. For 3-alkyl-1,8-naphthyridines, this active methylene component is an aliphatic aldehyde. To our knowledge, there is no previous work about the synthesis of compounds with the structure of **2c-e**, so this report may be the earliest on the use of aliphatic aldehydes to obtain this heterocyclic nucleus [14].

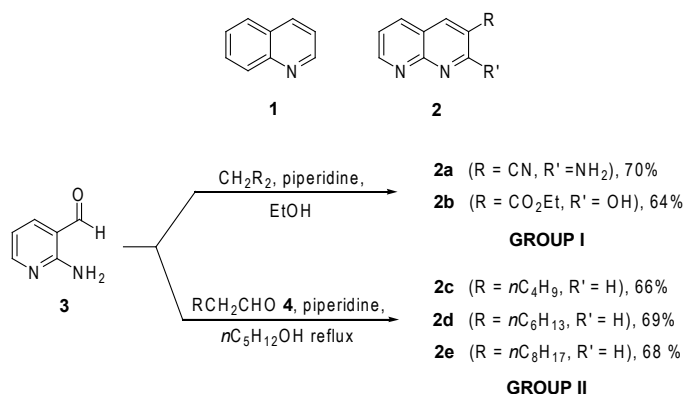


Fig. 1. Synthesis of Group I and Group II 1,8-naphthyridines.

The inhibiting properties of the five compounds were evaluated by Electrochemical Impedance Spectroscopy (EIS), a nominally non-destructive technique, on samples of API X52 carbon steel pipelines immersed in oilfield-related water. Results are expressed as Inhibition Efficiency (IE%), a significant parameter used to estimate the inhibitory activity.

## Results and discussion

### Synthesis of inhibitors

All 1,8-naphthyridines were prepared from commercially available compound **3**; alternatively, it can be also synthesized from ammonium sulfamate and nicotinamide [15]. For Group I 1,8-naphthyridines the active methylene component  $\text{CH}_2\text{Z}_2$  was malononitrile for **2a**, and diethyl malonate for **2b** [16] (Fig. 1). Both reactions proceed under smooth conditions; analytical data for these known substances were consistent with those reported on existing literature [17]. Preparation of Group II 1,8-naphthyridines requires relatively vigorous conditions (reflux in pentanol), but yields are acceptable (see below). Non-commercially available aldehydes **4** were prepared from the oxidation of the corresponding alcohol with PCC [18].

Structures for **2c-e** were unequivocally identified by spectrometric routine analyses. In  $^1\text{H}$  and  $^{13}\text{C}$  NMR analyses the signal assignments for the key compound **2c** were firmly established by COSY, DEPT and HETCOR experiments. Fragmentation pattern for this compound, shown in Figure 2, is proposed based on its mass spectrum, which is compliant with those reported for 3-alkylpyridines and related heterocycles [19]. Therefore, in addition to the molecular ion  $\text{M}^+$  ( $m/z$  186), McLafferty ( $m/z$  144),  $\beta$ -cleavage ( $m/z$  143, base peak) and fragments from loss of HCN were observed. Peaks for chain fragmentation are also present ( $m/z$  171 and 157) with a reasonable contribution—as can be theoretically predicted. In mass spectra of **2d** and **2e** McLafferty and  $\beta$ -cleavages are relevant, but  $m/z$  157 increases markedly to become the second largest peak (above  $m/z$  144) for **2d**, and it turns into the base peak for **2e**,  $m/z$  157 can be regarded as the product of a  $\gamma$ -cleavage,

and there is a remarkable parallel between this tendency and the one exhibited by 3-alkylpyridines with a long aliphatic chain [20], a conclusive fact that supports the proposed Group II 1,8-naphthyridines structure. A fragmentation mechanism is suggested for which, besides the generation of  $m/z$  157, a cyclic neutral structure is formed: a cyclobutane ring for **2d** and methylcyclopentane for **2e** (Fig. 3). Additional studies are now in progress to prepare 3-alkyl-1,8-naphthyridines with more complex groups for further understanding of this behavior.

### Electrochemical analysis of inhibitors

The inhibiting properties of the five new synthesized compounds were ascertained according to the qualitative/quantitative analyses of the impedance response spectra from EIS experiments. For these experiments, working electrodes were fabricated from API X52 carbon steel and immersed for 3h at 45 °C in the corrosive medium, that is, an oilfield-related water (**W**) sample (extracted from an authentic heavy crude oil) that was prepared to contain 500 ppm of each compound tested. For the five compounds a vehicle (methanol) was used to achieve this concentration (see experimental section). Individual impedance spectra were obtained for the five compounds and

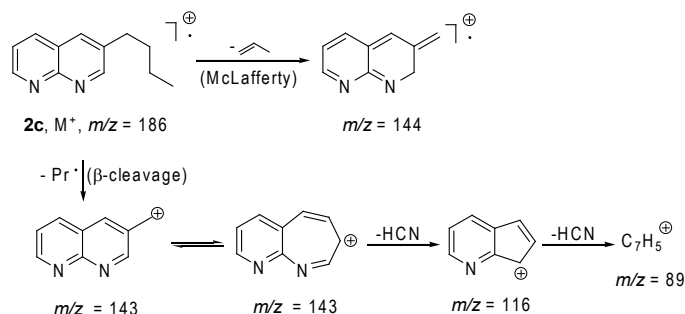


Fig. 2. Proposed fragmentation pattern for **2c**.

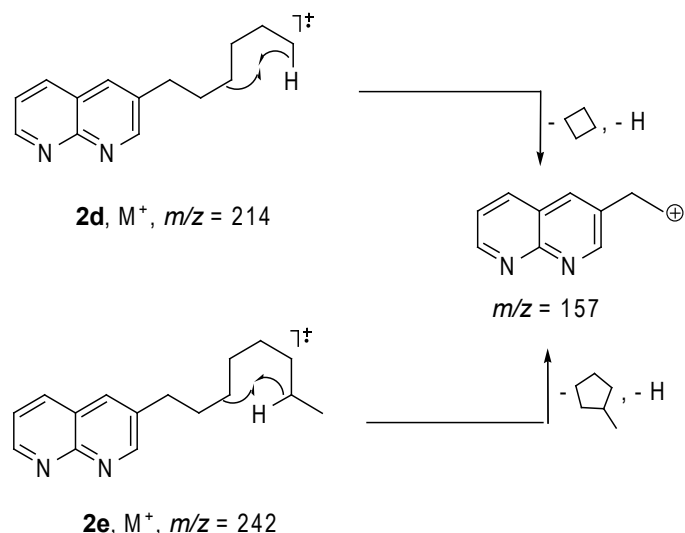


Fig. 3. Proposed fragmentation for **2d** and **2e**.

subsequently analyzed to determine their inhibition efficiency. About the qualitative analysis, Figure 4 exhibits the Nyquist, Bode module, and Bode-phase angle diagrams for water **W** only and the test solutions (**W** + 500 ppm of every inhibitor).

In the Nyquist diagram, Figure 4(a), when the real ( $Z_{\text{real}}$ ) and imaginary ( $-Z_{\text{imag}}$ ) components of complex impedance  $Z$  are plotted a depressed semicircle (or capacitive loop) is drawn, which for every inhibitor is of a larger diameter than that for water **W** only. In general, this implies that less electrons or ions are transferred through the interface, that is, larger impedance magnitudes create less interface activity, so the corrosion rate is decreased [21-23]. Therefore, it is plain that the five inhibitors cause an improved behavior against corrosion. In the Bode-module diagram, Figure 4(b),  $Z$  magnitudes (expressed as the logarithm of  $|Z|$ ) for all inhibitors are larger than the magnitude for **W**, so the enhanced anti-corrosion behavior discussed above is corroborated. Also a graphical inspection of the plot provides valuable information on the particularities of the corrosion process in the frequency  $f$  (or time) domain represented in the X-axis. For example, a horizontal line is an indication of a resistive interface behavior along the observed frequency interval, whereas a left sloped line of a capacitive behavior [24]. Hence, notice in Figure 4(b) that for all the inhibitors the high frequency plot segment is a relatively horizontal line, denoting that the presence of each compound creates variations in the test solution resistance. In addition, each physical phenomenon involved in the overall corrosion process can be identified when the plot slope changes [25]. Thus, observe in the figure that all plots possess two slope changes, implying that corrosion processes for the five inhibitors evolve according to two distinct physical phenomena: the first one (adsorption effect) emerges at high and intermediate frequencies and is originated by the “layer” of adsorbed inhibitor molecules formed on the X52 carbon steel surface; and the second (faradaic effect) appears at intermediate and low frequencies and can be related to the charge transfer resistance and charging of the double layer that are produced by bare (uncovered) steel sites not covered by the adsorbed layer of molecules [26].

Relevant supplementary knowledge can be attained from a scrutiny of the Bode-phase angle diagram, Figure 4(c). In graphic way, a capacitive behavior is recognized by a mountain-like plot shape that is height-dependant: lower heights

demonstrate less capacitive/more resistive interfaces (thus indicating lower corrosion rates), and vice versa [27]. Therefore, Figure 4(c) reveals that, consistent with the facts explained in the previous paragraphs, inhibitor **2d** behaves slightly more capacitive than water **W**, explicitly, corrosion rate is slightly modified, whereas inhibitors **2a-c** and **2e** cause more resistive behaviors that provoke smaller corrosion rates. Notice in the plot for **2c** and less obvious for **2e** two individual mountain-like shapes that provide evidence of the differentiated adsorption and faradaic effects: the first (adsorption) comes out at high frequencies, and afterward the second (faradaic) appears at lower frequencies. As a consequence, it can be suggested that the tested inhibitors act selectively in favor of either adsorption, faradaic, or both effects.

Concerning the quantitative analysis of spectra, it is worth mentioning that EIS is an interpretative technique that essentially needs that laboratory results be numerically fitted to match closely a pre-selected model [28]. This model, called “equivalent circuit” (EC), is shown in Figure 5. The electric elements and their notation for the EC are as follows:  $R_s$  is the resistance of the test solution (each new inhibitor dissolved in water **W**);  $R_a$  is the resistance of the layer of adsorbed molecules on the steel surface, and  $\text{CPE}_a$  is the Constant Phase Element (CPE, -a circuit element commonly used to account for non-ideal capacitive interfacial behaviors) [29] related to the capacitance of this layer. Moreover, the elements intended to model the bare steel surface properties are:  $R_{ct}$  (the charge transfer resistance), and  $\text{CPE}_{dl}$  (the CPE linked to the electric double layer capacitance). Based on the above, the impedance spectra were fitted for water **W** and the five inhibitors by a customary non-linear software [30] to find the EC electric component parameters (resistances and capacitances). Afterward, from these parameters and for the specific purposes of this work, overall resistances  $R_W$  and  $R_{inh}$  were determined for water **W** only and every inhibitor, respectively. Now, considering that the corrosion current is directly proportional to  $R_W^{-1}$  and  $R_{inh}^{-1}$ , the Inhibition Efficiency (IE%) was estimated according to  $100 \times [1 - (R_W/R_{inh})]$ . The results are presented in Table 1. With the aim of comparing the new inhibitor efficiencies, a commercial field-tested imidazoline-base corrosion inhibitor “CI” was arbitrarily thought of as a reference [31-32]; its calculated IE was 62.6% (see Table 1).

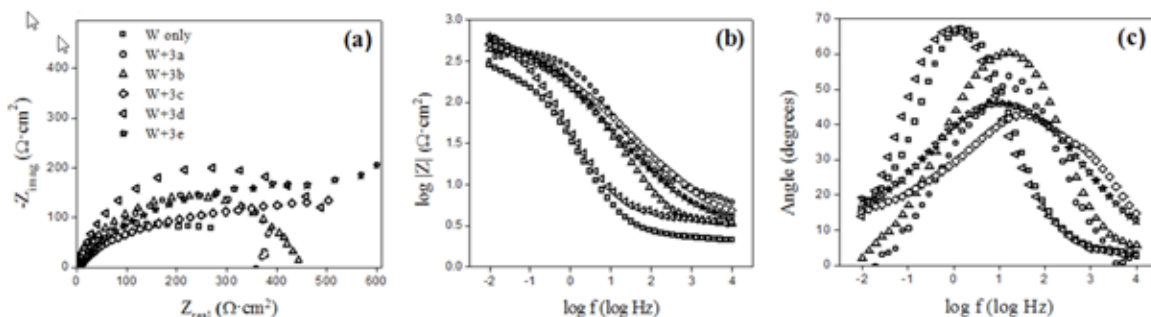


**Fig. 4.** (a) Nyquist, (b) Bode-module, and (c) Bode-phase diagrams of X52 carbon steel in water **W** and test solutions (water **W** + 500 ppm of each of the inhibitors shown).

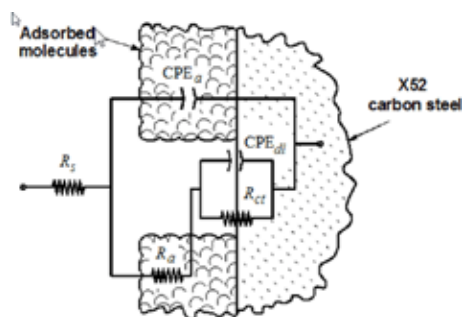


Fig. 5. Equivalent circuit (EC) used to fit experimental data.

The table shows that IE values found for the five new inhibitors are greater than that for the commercial CI. Additionally, except for **2d**, improvements in the order of 36 units (%) above the reference IE were achieved for the inhibitors. In summary, the inhibitory capabilities of the newly synthesized compounds were noteworthy, and hence their utilization as inhibitors can be promising in controlling inner corrosion of steel pipelines.

#### Feasible corrosion inhibition mechanism for 1,8-naphthyridines

1,8-naphthyridines can be recognized as bidentate alkaloids whose structural features are also present in other active related compounds, such as piperidines [33], 4,5-diphenyl-1-vinylimidazoles [34], and Schiff bases of ethylenediamine [35]. Based on the adsorption effect discussed previously in the electrochemical results, a percentage of the inhibitory activity for 1,8-naphthyridines can be explained if achelate effect [36] on the metal surface is considered (Fig. 6). This phenomenon would modify the electrode potential for oxidation, and thereby a decrement of the corrosion rate can occur. We are currently conducting experimental work to explore this proposal.

## Conclusions

Preliminary results indicate that significant corrosion inhibitory activity was found for four of the 1,8-naphthyridine tested under the described experimental conditions. Despite the remark-

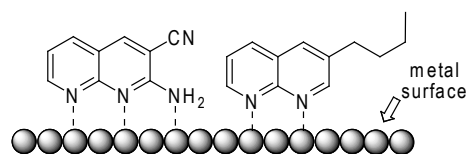


Fig. 6. Chelating bond proposed for **2a** (left) and **2c** (right) on the metal surface.

able differences between the electronic nature of Group I and Group II 1,8-naphthyridines, a minor variation in IE% values was found between the active compounds of both groups.

Although analyses with longer alkyl chain 3-alkyl-1,8-naphthyridines are needed, it may be very convenient to carry out studies on 1,8-naphthyridines with other functional groups. On the other hand, results in this work show that, albeit reaction conditions are somewhat rigorous, compounds with only one electron-withdrawing group as the aliphatic aldehydes **4** can be suitable raw materials to perform an extended Friedländer synthesis to prepare the 1,8-naphthyridine nucleus.

## Experimental Section

**General.** Infrared analyses were done with a Nicolet model Nexus 479 IR spectrometer. NMR experiments were carried out in a Jeol mod. Eclipse 300 spectrometer at room temperature in  $\text{CDCl}_3$ . EIMS spectra were recorded in a Jeol-JMX AX-505 WA spectrometer (70 eV). HRMS was measured in a JeolGC-Matell (EI, 70 eV) with per fluorokerosene as inner reference. Ion composition of oilfield-related water **W** was determined by High Performance Liquid Chromatography (HPLC) using a Dionex liquid-expert chromatographer. EIS experiments were done using an Autolab model PGSTAT30 potentiostat/galvanostat. System response and data processing were achieved with a frequency response analyzer (FRA) software.

**Chemical composition of oil field-related water W.** A standard chemical analysis was performed to a number of field-sampled water volumes; the resulting elements and their average concentration [in ppm] are as follows: Na [30,000]; K [3,445]; Ca [1,980]; Mg [1,245]; Mn [6.25]; Sr [1,388]; Ba [52.1]; Fe [0.22]; Cl [11,510];  $\text{SO}_4$  [2,930];  $\text{NO}_3$  [2,810]; F [121]. Measured pH was 7.20. This water was used as the solvent wherein every inhibitor was dissolved to attain 500 ppm concentration.

**2-Amino-3-cyano-1,8-naphthyridine (2a).** To a solution of 572 mg (8.66 mmol) of malononitrile in 3 mL of EtOH, 529 mg (4.33 mmol) of **3** were added. The reaction mixture was ice-cooled and 80  $\mu\text{L}$  of piperidine were added. The ice bath was removed and the reaction was stirred at room temperature overnight. Then, 30 mL of a  $\text{HCl}/\text{H}_2\text{O}$  6:4 v/v solution were added, and the reaction mixture was extracted twice with AcOEt (40 mL). Neutralization with  $\text{Na}_2\text{CO}_3$  of the aqueous phase and re-crystallization from EtOH of the formed solid produces 515 mg (3.03 mmol, yield: 70%) of the product. mp: 271–273  $^\circ\text{C}$  (reported 272–274  $^\circ\text{C}$ ). Spectroscopic analyses

Table 1. Inhibition efficiency (IE%) of the new inhibitors and CI.\*

Inhibitor	IE (%)
<b>2a</b>	99
<b>2b</b>	98.8
<b>2c</b>	99.1
<b>2d</b>	67.5
<b>2e</b>	99.5
CI	62.6

\* 500 ppm concentration; CI = commercial inhibitor.

(IR,  $^1\text{H}$  and  $^{13}\text{C}$  NMR, and MS-IE) were consistent with those reported on literature.

**2-Hydroxy-3-carbethoxy-1,8-naphthyridine (2b).** To a solution of 858 mg (5.36 mmol) of diethyl malonate in 2 mL of EtOH, 327 mg (2.68 mmol) of **3** and 50  $\mu\text{L}$  of piperidine were added. The reaction mixture was stirred for 5 days at room temperature. An isolation procedure as in **2a** was followed, and as a result 374 mg (1.71 mmol, 64%) of the product were obtained.  $\mu\text{p}$ : 207  $^\circ\text{C}$  (reported 205-207  $^\circ\text{C}$ ). Spectroscopic analyses (IR,  $^1\text{H}$  and  $^{13}\text{C}$  NMR, and MS-IE) were consistent with those reported on literature.

### General procedure for 3-alkyl-1,8-naphthyridines (2c-2e)

A mixture of the corresponding aliphatic aldehyde, **3**, piperidine, and pentanol was refluxed for 2.5 h. The excess of solvent was eliminated under reduced pressure, and the residue was then purified by flash column chromatography (AcOEt/hexane 1:1 v/v in Mallinkrodt Baker silica gel, 60-200 mesh) to obtain the product.

**3-Butyl-1,8-naphthyridine (2c).** Colorless oil (170 mg, 66%). IR (neat)  $\nu_{\text{max}}$  ( $\text{cm}^{-1}$ ): 2957, 2926, 2859, 1606, 1570, 1473, 1124, 785, 728.  $^1\text{H}$  NMR ( $\text{CDCl}_3$ , 300 MHz)  $\delta$  0.96 (t, 3 H,  $\text{CH}_3$ ,  $J = 7.4$  Hz), 1.41 (sext, 2 H- $\gamma$ ,  $J = 7.4$  Hz), 1.72 (q, 2 H- $\beta$ ,  $J = 7.4$  Hz), 2.83 (t, 2 H- $\alpha$ ,  $J = 7.7$  Hz) [ $\text{H}_{\text{aliph.}}$ ]; 7.47 (dd, H-6,  $J_1 = 8.2$  Hz,  $J_2 = 4.4$  Hz), 7.95 (d, H-4,  $J = 2.2$  Hz), 8.14 (dd, H-5,  $J_1 = 8.2$  Hz,  $J_2 = 1.9$  Hz), 8.99 (d, H-2,  $J = 2.2$  Hz), 9.06 (dd, H-7,  $J_1 = 4.1$  Hz,  $J_2 = 1.9$  Hz) [ $\text{H}_{\text{arom.}}$ ].  $^{13}\text{C}$  NMR ( $\text{CDCl}_3$ , 75 MHz)  $\delta$  13.87 ( $\text{CH}_3$ ), 22.25 (C- $\gamma$ ), 32.67 (C- $\alpha$ ), 33.11 (C- $\beta$ ) [ $\text{C}_{\text{aliph.}}$ ]; 122.11 (C-6), 122.62 (C-4a), 134.92 (C-4), 136.65, 136.72 (C-3 and C-5), 152.61 (C-7), 155.02 (C-8a), 155.32 (C-2) [ $\text{C}_{\text{arom.}}$ ]. MS (70 eV, EI):  $m/z$  (%): 186 [ $\text{M}]^+$  (95), 171 (4), 157 (9), 144 (71), 143 (100), 116 (54), 89 (27). HRMS (70 eV):  $m/z$ : Calcd. for  $\text{C}_{12}\text{H}_{14}\text{N}_2$ : 186.1157. Found: 186.1159.

**3-Hexyl-1,8-naphthyridine (2d).** Colorless gum (206 mg, 69%). IR (neat)  $\nu_{\text{max}}$  ( $\text{cm}^{-1}$ ): 2952, 2927, 2849, 1601, 1561, 1483, 1129, 795, 733.  $^1\text{H}$  NMR ( $\text{CDCl}_3$ , 300 MHz)  $\delta$  0.88 (t, 3 H,  $\text{CH}_3$ ,  $J = 7.14$  Hz); 1.33 (m, 6 H); 1.72 (q, H- $\beta$ ,  $J = 7.4$  Hz); 2.82 (t, H- $\alpha$ ,  $J = 7.7$  Hz) [ $\text{H}_{\text{aliph.}}$ ]; 7.47 (dd, H-6,  $J_1 = 8.2$  Hz,  $J_2 = 4.1$  Hz), 7.95 (d, H-4,  $J = 2.5$  Hz), 8.16 (dd, H-5,  $J_1 = 8.2$  Hz,  $J_2 = 1.9$  Hz), 8.99 (d, H-2,  $J = 2.2$  Hz), 9.07 (dd, H-7,  $J_1 = 4.1$  Hz,  $J_2 = 1.9$  Hz) [ $\text{H}_{\text{arom.}}$ ].  $^{13}\text{C}$  NMR ( $\text{CDCl}_3$ , 75 MHz)  $\delta$  14.15, 22.63, 28.90, 31.03, 31.67, 33.04 [ $\text{C}_{\text{aliph.}}$ ]; 122.22, 122.72, 135.08, 136.83, 136.88, 152.64, 154.92, 155.34 [ $\text{C}_{\text{arom.}}$ ]. MS (70 eV, EI):  $m/z$  (%): 214 [ $\text{M}]^+$  (34), 199 (3), 185 (8), 171 (32), 157 (91), 144 (85), 143 (100), 116 (40), 89 (19). HRMS (70 eV):  $m/z$ : Calcd. for  $\text{C}_{14}\text{H}_{18}\text{N}_2$ : 214.1470. Found: 214.1471.

**3-Octyl-1,8-naphthyridine (2e).** Colorless gum (229 mg, 68%). IR (neat)  $\nu_{\text{max}}$  ( $\text{cm}^{-1}$ ): 2962, 2927, 2850, 1602, 1566, 1463, 1124, 805, 728.  $^1\text{H}$  NMR ( $\text{CDCl}_3$ , 300 MHz)  $\delta$  0.88 (t,  $\text{CH}_3$ ,  $J = 6.9$ ); 1.32 (m, 10 H); 1.72 (q, 2 H- $\beta$ ,  $J = 6.9$  Hz); 2.82 (t, 2 H- $\alpha$ ,  $J = 7.7$  Hz) [ $\text{H}_{\text{aliph.}}$ ]; 7.48 (dd, H-6,  $J_1 = 8.2$  Hz,  $J_2 = 4.1$  Hz), 7.96 (d, H-4,  $J = 1.9$  Hz), 8.16 (dd, H-5,  $J_1 = 8.2$  Hz,  $J_2 = 1.6$  Hz), 9.01 (d, H-2,  $J = 1.6$  Hz), 9.08 (m, H-7) [ $\text{H}_{\text{arom.}}$ ].  $^{13}\text{C}$  NMR ( $\text{CDCl}_3$ , 75 MHz)  $\delta$  14.10, 22.64, 29.16, 29.19, 30.99,

31.82, 31.88, 32.96 [ $\text{C}_{\text{aliph.}}$ ]; 122.17, 122.64, 135.05, 136.78, 136.86, 152.56, 154.69, 155.23 [ $\text{C}_{\text{arom.}}$ ]. MS (70 eV, EI):  $m/z$  (%): 242 [ $\text{M}]^+$  (10), 213 (6), 199 (16), 185 (14), 171 (40), 157 (100), 144 (98), 143 (36), 116 (22), 89 (13). HRMS (70 eV):  $m/z$ : Calcd. for  $\text{C}_{16}\text{H}_{22}\text{N}_2$ : 242.1783. Found: 242.1781.

### Acknowledgments

Thanks are given to Dr. Eleuterio Burgueño-Tapia (Escuela Nacional de Ciencias Biológicas, Instituto Politécnico Nacional) for his assistance.

### References

- Ahmad, Z. *Principles of corrosion engineering and corrosion control*. Elsevier LTD: Great Britain, 2006. pp. 325-981.
- D. A. Jones. *Principles and prevention of corrosion*. 2<sup>nd</sup>. Ed. Prentice Hall, Inc.: U. S. A., 1996. pp. 477-512.
- Uhlig, H. H.; Revie, R. W. *Corrosion and corrosion control. An introduction to corrosion science and engineering*. 3<sup>rd</sup>. Ed. J. Wiley & Sons, Inc. U. S. A., 1985. pp. 263-277.
- Abdel-Aal, M. S.; Ahmed, Z. A.; Hassan, M. S. *J. Appl. Electrochem.* **1992**, 22, 1104-1109.
- Skrypnik, Y. G.; Doroshenko, T. F. *Mater. Sci.* **1996**, 32, 537-544.
- Achary, G.; Sachin, H. P.; Arthoba Naik, Y.; Venkatesha, T. V. *Mater. Chem. Phys.* **2008**, 107, 44-50.
- Ebenso, E. E.; Obot, I. B.; Murulana, L. C. *Int. J. Electrochem. Sci.* **2010**, 5, 1574-1586.
- Lowe, P. A. in *Comprehensive heterocyclic chemistry. The structure, reactions, synthesis and use of heterocyclic compounds*. Katritzky, A.; Rees, C. W., Eds.; Pergamon Press Ltd.: Great Britain, 1984; Vol. 2, pp. 581-627.
- Stanforth, S. P. in *Comprehensive heterocyclic chemistry II. A review of the literature 1982-1995*. Katritzky, A.; Rees, C. W.; Scriven, E. F. V., Eds.; Elsevier Science Ltd.: Great Britain, 1996. Vol. 7, pp. 527-559.
- Dobbs, A. P. in *Comprehensive heterocyclic chemistry III. A review of the literature 1995-2007*. Katritzky, A.; Ramsden, C. A.; Scriven, E. F. V.; Taylor, R. J. K., Eds.; Elsevier Ltd.: Great Britain, 2008. Vol. 7, pp. 713-715.
- Cheng, C.C.; Yan, S.-J. *Org. React.* **1982**, 28, 37-201.
- Paquette, L. A. *Encyclopedia of reagents for organic synthesis*. John Wiley & Sons, Ltd.: England, 1995. Vol. 1, pp. 184-185.
- Many substrates have been utilized as active methylene component, in acid and in basic media; see Thummel, R. P.; Lefoulon, F.; Cantu, D.; Mahadevan, R. *J. Org. Chem.* **1984**, 49, 2208-2212. The practice of  $\text{KI}_3$  catalysis has also been reported: Mogilaiah, K.; Kumar, K. S.; Reddy, N. V. *Indian J. Chem.* **2010**, 49B, 253-255.
- Active methylene components also yield 1,8-naphthyridines in presence of other substrates. See Higashino, T.; Suzuki, K.; Hayashi, E. *Chem. Pharm. Bull.* **1978**, 26, 3242-3243.
- Majewicz, T. G.; Caluwe, P. *J. Org. Chem.* **1974**, 39, 720-721.
- Actually, IR analysis is rather consistent with the presence of the keto tautomer for **2b** ( $\nu = 1704 \text{ cm}^{-1}$ ). Nevertheless, its representation as the 2-hydroxy compound is depicted for simplicity purposes.
- Hawes, E. M.; Wibberley, D. G. *J. Chem. Soc. C* **1966**, 315-321.
- Corey, E. J.; Suggs, J. W. *Tetrahedron Lett.* **1975**, 31, 2647-2650.

19. Budzikiewicz, H.; Djerassi, C.; Williams, D. H. *Mass spectrometry of organic compounds*. Holden-Day Inc. U. S. A., 1967. pp. 566-595.
20. Mass spectrum for 3-butylpyridine is available online in [http://riodb01.ibase.aist.go.jp/sdbs/cgi-bin/direct\\_frame\\_top.cgi](http://riodb01.ibase.aist.go.jp/sdbs/cgi-bin/direct_frame_top.cgi). For 3-hexyl- and 3-octylpyridine, see Thomas, A. F.; Bassols, F. *J. Agric. Food Chem.* **1992**, *40*, 2236-2243.
21. Freire, L.; Carmezim, M. J.; Ferreira, M. G. S.; Montemor, M. F. *Electrochim. Acta* **2011**, *56*, 5280-5289.
22. Acevedo-Peña O.; Vázquez G.; Laverde, D.; Pedraza-Rosas, J. E.; González, I. *J. Solid State Electrochem.* **2010**, *14*, 757-767.
23. Lin, P.-Ch.; Sun, I.-W.; Chang, J.-K.; Su, Ch.-J.; Lin, J.-Ch. *Corros. Sci.* **2011**, *53*, 4318-4323.
24. Orazem, M. E.; Tribollet, B. *Electrochemical impedance spectroscopy*. John Wiley & Sons, Inc. U. S. A., 2008. pp. 61-72.
25. Hernández, R. del P. B.; Aoki, I. V.; Tribollet, B.; de Melo, H. G. *Electrochim. Acta* **2011**, *56*, 2801-2814.
26. Mendoza-Canales, J.; Marín-Cruz, J. *J. Solid State Electrochem.* **2008**, *12*, 1637-1644.
27. Marín-Cruz, J.; Cabrera-Sierra, R.; Pech-Canul, M. A. *J. Solid State Electrochem.* **2007**, *11*, 1245-1252.
28. Bard, A. J.; Inzelt, G.; Scholz, F. *Electrochemical dictionary*. Springer: Berlin, 2008. pp. 188-189.
29. Toledo-Matos, L. A.; Pech-Canul, M. A. *J. Solid State Electrochem.* **2011**, *15*, 1927-1934.
30. ZView Version 3.2b. Copyright © 1990-2010, Scribner Associates, Inc., written by Derek Johnson.
31. Feng, L.; Yang, H.; Wang, F. *Electrochim. Acta* **2011**, *58*, 427-436.
32. Ortega-Toledo, D. M.; González-Rodríguez, J. G.; Casales, M.; Martínez, L.; Martínez-Villafañe, A. *Corros. Sci.* **2011**, *53*, 3780-3787.
33. Khaled, K. F.; Babić-Samardžija, K.; Hackerman N. *J. Appl. Electrochem.* **2004**, *34*, 697-704.
34. Wahyuningrum, D.; Achmad, S.; Syah, Y. M.; Buchari; Bundjali, B.; Ariwahjoedi, B. *Int. J. Electrochem. Sci.*, **2008**, *3*, 154-166.
35. Agrawal, Y. K.; Talati, J. D.; Shah, M. D.; Desai, M. N.; Shah, N. K. *Corros. Sci.* **2004**, *46*, 633-651.
36. Huheey, J. E.; Keiter, E. A.; Keiter, R. L. *Inorganic chemistry. Principles of structure and reactivity*. 4<sup>th</sup>. Ed. HarperCollins College Publishers: U. S. A., 1996. pp. 522-531.